

This discussion paper is/has been under review for the journal Atmospheric Chemistry and Physics (ACP). Please refer to the corresponding final paper in ACP if available.

Aerosol physical and chemical properties retrieved from ground-based remote sensing measurements during heavy haze days in Beijing winter

Z. Q. Li¹, X. Gu¹, L. Wang^{1,2}, D. Li^{1,3}, K. Li^{1,3}, O. Dubovik⁴, G. Schuster⁵, P. Goloub⁴, Y. Zhang^{1,3}, L. Li^{1,3}, Y. Xie^{1,3}, Y. Ma¹, and H. Xu¹

¹State Environmental Protection Key Laboratory of Satellites Remote Sensing, Institute of Remote Sensing and Digital Earth of Chinese Academy of Sciences, Beijing 100101, China

²International Institute for Earth System Science, Nanjing University, Nanjing 210093, China

³University of Chinese Academy of Sciences, Beijing, 100049, China

⁴Laboratoire d'Optique Atmosphérique, Université Lille 1, Villeneuve d'Ascq 59655, France

⁵NASA Langley Research Center, Hampton, VA 23681, USA

Received: 29 January 2013 – Accepted: 6 February 2013 – Published: 21 February 2013

Correspondence to: L. Wang (wl8394722@126.com)

Published by Copernicus Publications on behalf of the European Geosciences Union.

Title Page

Abstract

Introduction

Conclusions

References

Tables

Figures

◀

▶

◀

▶

Back

Close

Full Screen / Esc

Printer-friendly Version

Interactive Discussion



Abstract

With the development of economy in the past thirty years, many large cities in the eastern and southwestern China are experiencing increased haze events and atmospheric pollution, causing significant impacts on the regional environment and even climate. However, knowledge on the aerosol physical and chemical properties in heavy haze conditions is still insufficient. In this study, two winter heavy haze events in Beijing occurred in 2011 and 2012 were selected and investigated by using the ground-based remote sensing measurements. We used CIMEL CE318 sun-sky radiometer to derive haze aerosol optical, physical and chemical properties, including aerosol optical depth (AOD), size distribution, complex refractive indices and fractions of chemical components like black carbon (BC), brown carbon (BrC), mineral dust (DU), ammonium sulfate-like (AS) components and aerosol water content (AW). The retrieval results from a total of five haze days showed that the aerosol loading and properties during the two winter haze events were relatively stable. Therefore, a parameterized heavy haze characterization was drawn to present a research case for future studies. The averaged AOD is 3.2 at 440 nm and Ångström exponent is 1.3 from 440–870 nm. The coarse particles occupied a considerable fraction of the bimodal size distribution in winter haze events, with the mean particle radius of 0.21 and 2.9 μm for the fine and coarse mode respectively. The real part of the refractive indices exhibited a relatively flat spectral behavior with an average value of 1.48 from 440 to 1020 nm. The imaginary part showed obviously spectral variation with the value at 440 nm (about 0.013) higher than other three wavelengths (e.g. about 0.008 at 675 nm). The chemical composition retrieval results showed that BC, BrC, DU, AS and AW occupied 1 %, 2 %, 49 %, 15 % and 33 % respectively on average for the investigated haze events. The comparison of these remote sensing results with in situ BC and $\text{PM}_{2.5}$ measurements were also presented in the paper.

Aerosol physical and chemical properties

Z. Q. Li et al.

Title Page

Abstract

Introduction

Conclusions

References

Tables

Figures

◀

▶

◀

▶

Back

Close

Full Screen / Esc

Printer-friendly Version

Interactive Discussion



1 Introduction

Haze is an atmospheric optical phenomenon which leads to significant decrease of the atmospheric visibility due to the suspended solid or liquid particles, smoke, and vapor in the atmosphere. One major constituent of haze is aerosol particles, such as dust and soot from fuel or coal burning. Haze formation is thought to be closely related to meteorological conditions and air pollution (Sun et al., 2006; Lai and Sequeira, 2001). When haze occurs, environmental air is usually polluted and affects human health. In addition, it has significant effects on cloud formation and regional climate (Okada et al., 2001; Menon et al., 2002). In recent years, the haze pollution has drawn growing worldwide concerns, especially in developing countries. The rapid increase in energy consumption and amount of vehicles in the past three decades plus high population density have caused serious particulate matter (PM) pollution in Beijing (He et al., 2002). Haze event has been observed frequently in Beijing (Sun et al., 2006), during the cold winter and spring seasons because of the enhanced heating, traffic and industrial emissions and especially the stable weather conditions. Meanwhile, dust blow from local and the north arid region is still an unending phenomenon in Beijing during the dry winter and spring seasons. The mineral dust component further mixing with local aerosols makes the nature of haze aerosols in Beijing distinct from others. However, studies on the haze pollution in Beijing are rather limited and simultaneous observation of physical and optical properties as well as the chemical characteristics of haze aerosol are even less.

In this paper, two haze events occurring in the winter time of February 2011 and 2012 over Beijing were studied. We measured attenuation of direct solar beam and sky radiation distribution by using a new generation CIMEL polarized sun-sky radiometer to derive accurate aerosol optical depth (AOD) and comprehensive aerosol properties like particle size distribution, single scattering albedo (SSA) and refractive indices (Holben et al., 1998; Dubovik et al., 2000, 2006). These aerosol optical and microphysical parameters provide a base for retrieval of the aerosol chemical composition informa-

Title Page

Abstract

Introduction

Conclusions

References

Tables

Figures

◀

▶

◀

▶

Back

Close

Full Screen / Esc

Printer-friendly Version

Interactive Discussion



tion, which allows the estimate of the aerosol component fraction without destroying the ambient status of atmospheric particles.

2 Measurement and methodology

2.1 Observation site and instrument

5 In this study, the observation site (116.37° E, 40.00° N) in Beijing is located on the building roof (~ 59 m a.s.l.) of the Institute of Remote Sensing and Digital Earth, Chinese Academy of Sciences. The instrument we used is a CIMEL CE318-DP sun-sky radiometer, #350 in the AEROSOL ROBOTIC NETWORK (AERONET) (Holben et al., 1998). It has eight wavelengths, nominally centered at 340, 380, 440, 500, 675, 870, 1020
10 and 1640 nm with bandwidth from 2 to 10 nm for the purpose of aerosol observation. Measurements are automatically scheduled with direct sun irradiance measurements of about each 10 min and angular sky radiance scanning of about each one hour. In practice, the direct sun attenuation measurements are performed in a triplet way within about 30 s which can be used to detect clouds (Smirnov et al., 2000). Sky scanning
15 in almucantar and solar principle plan (SPP) geometry for intensity and polarization measurements can be used to retrieve aerosol optical, physical and chemical properties. The sky measurements are performed wavelength by wavelength, costing about 5–8 min depending on instrument scenario and wavelengths appointed by the user. Calibration of the direct sun measurements of the radiometer (#350) was made by inter-
20 calibration with the AERONET master instrument (#245) on 2 November 2009, and the high mountain Langley calibration at Litang site (3913 m) on 13 October 2011, respectively. The sky radiance was calibrated following the vicarious method (Li et al., 2008). The polarization calibration was performed in the laboratory on 28 October 2009. The measurement uncertainty and calibration precision can be found in the AERONET web
25 and Holben et al. (1998).

Title Page

Abstract

Introduction

Conclusions

References

Tables

Figures

◀

▶

◀

▶

Back

Close

Full Screen / Esc

Printer-friendly Version

Interactive Discussion



2.2 Two haze events in Beijing winter

Haze can cause sky dimming, and thus numerous studies propose to use the visibility as a proxy to identify the haze event (e.g. Bäumer et al., 2008). Here, we consider a three-parameter criteria to select haze from our measurements, which includes AOD (440 nm) > 1.0, Ångström exponent α > 1.0 and the Relative Humidity (RH) < 90%. Firstly, AOD has a relationship with visibility and the AOD (440 nm) greater than 1.0 corresponds to approximately a visibility lower than about 5 km in the standard atmospheric model, which can be recognized as heavy haze. Secondly, the threshold on α is set to distinguish haze from the dust storm cases which can also have high AOD values, but usually with a much lower α . Thirdly, the ambient humidity criterion is useful to distinguish fog from haze conditions (Wu et al., 2005). According to these criteria, we selected two typical haze events during 22–23 February 2011 and 27–29 February 2012 respectively. Figure 1 shows the measured AOD and Ångström exponent (440–870 nm) during the two haze events. In the first event (2011), the averaged AOD (440 nm) is about 4, while it is about 3 in the second event (2012). In 2012 event, the Ångström exponent is higher than 2011, indicating more small size particles. It should be noted that AOD at 440 nm may associate with much larger uncertainties than other three wavelengths due to reaching the measurement limitation of the CE318 instrument in these extremely heavy haze events.

2.3 Retrieval of aerosol physical properties

We utilize the comprehensive aerosol retrieval code developed by Dubovik et al. (2000, 2006) in this study, which is also the standard inversion algorithm for AERONET aerosol products. The retrieved aerosol property parameters include the particle size distribution and the wavelength dependent refractive indices as well as other aerosol optical parameters like SSA with error estimation. The algorithm employs the spheroid model (Volten et al., 2001) to improve the performance when dealing with coarse particles while the discrete ordinates method (Nakajima and Tanaka, 1988; Stamnes et al.,

Title Page

Abstract

Introduction

Conclusions

References

Tables

Figures

◀

▶

◀

▶

Back

Close

Full Screen / Esc

Printer-friendly Version

Interactive Discussion



1988) is used to solve the radiative transfer equation. In the retrieval, the ground reflectance is assumed to be Lambertian with albedo obtained from a five-year half-monthly averaged MODIS climatology (Li et al., 2006). We carry out cloud screening by using the triplet direct-sun measurement stability and the almucantar measurement asymmetry (Smirnov et al., 2000). In Fig. 2, we show an example to illustrate the fit of sky radiance (L) measurements based on the retrieved aerosol parameters. The residual ε is defined as

$$\varepsilon_L(\lambda; \Theta) = \frac{L^{\text{cal}}(\lambda; \Theta) - L^{\text{meas}}(\lambda; \Theta)}{L^{\text{meas}}(\lambda; \Theta)}, \quad (1)$$

where λ is the wavelength, Θ is the scattering angle, the superscript $^{\text{meas}}$ and $^{\text{cal}}$ denote the measured and calculated (using the retrieved aerosol parameters) sky radiance respectively. The radiance used in this study is normalized by π/E_0 with E_0 the extraterrestrial solar irradiance. The smaller sky radiance residual (comparable with the radiance calibration uncertainty of 3–5 %) suggests that the inversion algorithm performs well in the case of heavy haze events. Moreover, taking the advantage of the CE318-DP instrument, we can also verify the retrieval results in the heavy haze events by validating residuals on the independent degree of linear polarization (P) measurements following:

$$\varepsilon_P(\lambda; \Theta) = P^{\text{cal}}(\lambda; \Theta) - P^{\text{meas}}(\lambda; \Theta) \quad (2)$$

From Fig. 2, we find the residuals on P are less than 0.01 in average at all wavelengths (averaged for measurement angles), which agrees well with the calibration accuracy of the polarization measurements.

2.4 Retrieval of aerosol chemical composition

In general, aerosol is a complicated mixture of liquid water and dry components. According to the aerosol scattering and absorbing properties, the dry aerosol particles

Title Page

Abstract

Introduction

Conclusions

References

Tables

Figures

◀

▶

◀

▶

Back

Close

Full Screen / Esc

Printer-friendly Version

Interactive Discussion



Aerosol physical and
chemical properties

Z. Q. Li et al.

Title Page

Abstract

Introduction

Conclusions

References

Tables

Figures

◀

▶

◀

▶

Back

Close

Full Screen / Esc

Printer-friendly Version

Interactive Discussion



can be divided into two categories: first is the absorbing components like Black Carbon (BC), dust (DU) and the still poorly understood Brown Carbon (BrC) generated from combustion processes (Moosmuller et al., 2009); second the scattering (non-absorbing) components like sulfate, nitrate and sea salt etc. Here, we assume a mixture model of aerosols including 5 components, i.e. BC, BrC, DU, ammonium sulfate (AS) and water (AW) as shown in Fig. 3, considering that sea salt can be generally neglected in Beijing and the ammonium sulfate can be used as a proxy of non-absorbing dry components (Schuster et al., 2005; Arola et al., 2011). This model is an extension of the 3-component model of Schuster et al. (2005) and 4-component model of Arola et al. (2011). To apply this model to remote sensing measurement, we consider using information obtained from spectral variation of imaginary part of refractive index, and the spectral variation of SSA.

The averaged aerosol refractive indices over Beijing in 2010 are presented on the left panel of Fig. 4. The enhanced absorption (larger imaginary part) at 440 nm reveals the presence of spectrally depend absorbing aerosols like DU or BrC, while BC usually causes wavelength-independent absorption (Bond and Bergstrom, 2006). In order to include dust and BrC in the retrieval simultaneously, we consider using the size-dependent absorption parameter, i.e. the SSA (Dubovik et al., 2002), as DU and BrC usually have different particle size. In general, DU components are usually coarse particles, while BrC generated from combustion processes are typically fine particles. On the right panel of Fig. 4, we exhibit the averaged spectral SSA obtained from January to December 2010 over Beijing for periods with predominately coarse (Ångström Exponent $AE < 0.6$) and fine particles (Ångström Exponent $AE > 1.5$), respectively (Dubovik et al., 2002; Schuster et al., 2006). The SSA spectral trends from 675 and 870 nm show clearly difference (an increased pattern for coarse particles while a decreased pattern for fine particles), respectively for the two cases. We employ this behavior in our retrieval to help distinguish DU from BrC.

The detailed algorithm on the aerosol chemical composition retrieval is described in a paper recently submitted to JGR (Wang et al., 2013). Here, we provide a brief review

of this algorithm. In the estimation of aerosol chemical composition, aerosol parameters including refractive indices n (the real part) and k (the imaginary part), as well SSA for each of five components and the aerosol mixture should be known previously. The parameters of ambient aerosol mixture can be obtained from CE318 retrieval results and those of aerosol components are obtained from related literatures (e.g. Schuster et al., 2005; Dey et al., 2006; Arola et al., 2011). Then, the optical properties of aerosol mixture are calculated following Maxwell–Garnet effective medium approximation for the given volume fractions of the five components (Schuster et al., 2005; Wang et al., 2013). Finally, estimate of the volume fractions of the aerosol components is obtained when the calculated aerosol optical properties match best of the values retrieved from the sun photometer measurements, which equals to

Optimization of $\Psi(\varepsilon_n, \varepsilon_{k(\text{blue})}, \varepsilon_{k(\text{red})}, \varepsilon_{\text{dSSA}}) \rightarrow f_i (i = 1 \dots 5)$, with

$$\varepsilon_n = \frac{|n^{\text{cal}} - n^{\text{ret}}|}{n^{\text{ret}}},$$

$$\varepsilon_{k(\text{blue})} = \frac{|k_{\text{blue}}^{\text{cal}} - k_{\text{blue}}^{\text{ret}}|}{k_{\text{blue}}^{\text{ret}}},$$

$$\varepsilon_{k(\text{red})} = \frac{|k_{\text{red}}^{\text{cal}} - k_{\text{red}}^{\text{ret}}|}{k_{\text{red}}^{\text{ret}}},$$

$$\varepsilon_{\text{dSSA}} = \frac{|\text{dSSA}^{\text{cal}} - \text{dSSA}^{\text{ret}}|}{|\text{dSSA}^{\text{ret}}|},$$
(3)

where i is number index of chemical components, f_i denotes the volume fraction of each component in the mixture, n is obtained from spectral average of real part refractive indices at four wavelengths, k_{blue} is obtained from imaginary part of refractive

Title Page

Abstract

Introduction

Conclusions

References

Tables

Figures

◀

▶

◀

▶

Back

Close

Full Screen / Esc

Printer-friendly Version

Interactive Discussion



indices at 440 nm, k_{red} is obtained from average of imaginary part of refractive indices from 675 to 1020 nm, and dSSA is defined as $\text{SSA}(870 \text{ nm}) - \text{SSA}(675 \text{ nm})$. In the process of optimization of function ψ , in order to avoid problems on weighting four kinds of input information (n , $k(\text{blue})$, $k(\text{red})$ and dSSA), we utilize a “rank position priority” strategy, instead of using the traditional least square mean method. We calculate residual ε of each kind of information in the same f_i space. Then, for each kind of information, we number the f_i solutions according to the ε . The smaller ε , the smaller the rank number is (or the high priority position). At last, the best solution for all kinds of information can be found with the minimized summation of rank numbers accounted for all four kinds of information.

3 Results

3.1 Aerosol physical characteristics during haze events

3.1.1 Size distribution

Particles size distribution is a key aerosol physical parameter showing clearly the fine and coarse particle fractions in the atmosphere. Figure 5 shows the aerosol size distribution retrieved from sun-sky radiometer measurements during the two haze events. In the 2011 event, the absolute value on 23 February is higher than that of 22 February, which corresponds to higher AOD on 23 February as shown in Fig. 1. Meanwhile, the both obviously higher fine and coarse modes on 23 February cause an increase in AOD, while the Ångström exponent keeps stable compared to 22 February. In the 2012 event, it contains more coarse particles in fraction compared with 2011 cases. In the 2011 haze event, it contains 39% coarse particles in volume, while in the second event 48%. Moreover, in 2012 event, the fine mode contains much smaller particles compared with 2011 event. For example the central radius of fine mode varies from 0.16–0.2 μm in 2012 versus 0.23–0.26 μm in 2011 cases, which corresponds to higher

Title Page

Abstract

Introduction

Conclusions

References

Tables

Figures

◀

▶

◀

▶

Back

Close

Full Screen / Esc

Printer-friendly Version

Interactive Discussion



Ångström exponent of 2012 than 2011 in Fig. 1. In addition, following quite stable behavior of Ångström exponent of 2011 and 2012 events in Fig. 1, it is reasonable to derive the averaged size distribution for the two events. As illustrated in Fig. 6, the 2011 event has larger fine mode than 2012, but particle size of fine mode in 2012 event is smaller.

3.1.2 Refractive indices

Refractive indices are important physical parameters of aerosol particles and key indicators of aerosol chemical composition. The real part reflects the aerosol scattering property and reveals information about the water content in aerosols. For example, aerosol mixtures with refractive indices close to 1.33 have an abundance of water content, while those with refractive indices higher than 1.57 are nearly totally dry (Schuster et al., 2009). The imaginary part reflects the aerosol absorbing property and its spectral pattern can reveal the relative fractions of absorbing aerosols like BC and DU (Schuster et al., 2005; Russell et al., 2010; Wang et al., 2012).

In Fig. 7, we represent the daily averaged refractive indices during the two haze events in 2011 and 2012. The real parts for all cases exhibit relatively flat behaviors with the daily averaged values at four wavelengths concentrated between 1.45–1.51. Compared to the real parts, the imaginary parts show obviously spectral variation, with the 440 nm value significantly higher than that of other bands. The averaged refractive index during the haze events in 2011 and 2012 are shown in Fig. 8. The mean value of the real part at 675 nm is 1.50 in 2011 and 1.48 for 2012, which indicates more water content in 2012 event than 2011. The averaged imaginary parts at 440 are both 0.013 for the two events, while about 0.008 at 675 nm.

3.2 Aerosol chemical component fraction during haze events

Figure 9 shows the volume fractions of the five chemical components of BC, BrC, DU, AS, and AW for each day during the two haze events. The volume fractions of chemical

Title Page

Abstract

Introduction

Conclusions

References

Tables

Figures

◀

▶

◀

▶

Back

Close

Full Screen / Esc

Printer-friendly Version

Interactive Discussion



Aerosol physical and
chemical properties

Z. Q. Li et al.

Title Page

Abstract

Introduction

Conclusions

References

Tables

Figures

◀

▶

◀

▶

Back

Close

Full Screen / Esc

Printer-friendly Version

Interactive Discussion



components exhibit somewhat larger variations (represented by the error bar) within the day, probably caused by the change in the life time of different chemical components and the weather conditions (such as temperature, wind velocity and relative humidity). However, the mean volume fraction of each chemical component shows relatively small day-to-day variations ($< 10\%$) during each haze event, indicating that the aerosol sources are quite stable throughout each haze event. The averaged volume fraction of each chemical component for each haze event is presented in Fig. 10. From Fig. 10, one can find that although the haze events occurred in different years, the aerosol chemical composition fractions are comparable to each other with the difference in volume fraction less than 5% absolute. This is partly related to the consistent time period of the two events, i.e. both in winter.

Among the five components, the BC and BrC content show extremely low levels in all cases with no more than 2% and 5% respectively in the aerosol. During the two haze events, water occupies a relatively large fraction, ranging from 25% to 38%, with 2012 higher than 2011. From the water fraction, the geometric hygroscopic growth factor (gHGF) of aerosol can be inferred from a simple mathematical formula (Schuster et al., 2009). The gHGF of the 2011 haze event is 1.11, and 1.17 for the 2012 event. When gHGF is larger than 1.11, the aerosol is hygroscopic (Schuster et al., 2009), indicating that the aerosols can absorb moisture from the environment. Dust aerosols also occupy a large fraction in the aerosol during the haze events, and the volume fractions in the two events are both around 50%. The high dust content in winter time is likely due to local emission from arid land and ash emissions related to coal burning (Yang et al., 2009). Moreover, in situ chemical sampling measurements in Beijing during the wintertime also showed that the dust can account for 50% of the total aerosol mass concentrations at the surface (Duan et al., 2007; Yuan et al., 2008). The AS accounts for nearly 20% in the aerosol particles during the haze events. In this study, AS is the proxy for the scattering dry components in the aerosol, which are usually composed by water-soluble and water-insoluble components as well. Hence, it should be noted that AS retrieved in this study is different with the ammonium sulfate obtained by the

chemical sampling approaches, which is normally considered to include only the water-soluble component.

3.3 Averaged aerosol physical and chemical properties during winter heavy haze event in Beijing

From Sect. 3.1 to 3.2, we find stable aerosol properties during 5 days of the heavy haze events in two years. Therefore, it is reasonable to provide an averaged typical optical, physical and chemical model on heavy haze based on observations during the above two winter haze events in Beijing. As listed in Table 1, during the winter heavy haze events, the aerosols are characterized by large AOD (440 nm) about 3.22 ± 0.71 , with Ångström exponent of about 1.3, suggesting fine particle dominates the event. The aerosol size distributions are bimodal and the coarse mode occupies a considerable fraction, which is different from the haze events in southern China cities such as Guangzhou, where the fine particle ratio is generally much higher (Tan et al., 2009). The mean particle radius and the standard deviation are (0.21 μm , 0.51) and (2.9 μm , 0.65) for the fine and coarse modes respectively. With these parameters, the aerosol size distributions over Beijing for haze days can be modeled by bimodal lognormal function (Dubovik et al., 2002; Schuster et al., 2006):

$$\frac{dV(r)}{d\ln r} = \frac{C_f}{\sqrt{2\pi}\sigma_f} \exp\left[-\frac{(\ln r - \ln r_f)^2}{2\sigma_f^2}\right] + \frac{C_c}{\sqrt{2\pi}\sigma_c} \exp\left[-\frac{(\ln r - \ln r_c)^2}{2\sigma_c^2}\right], \quad (4)$$

where r is the particle radius, C_f and C_c denote the particle volume concentration for fine and coarse mode respectively, r_f and r_c are the median radius, and σ_f and σ_c are the standard deviation as listed in Table 1.

The refractive indices are 1.48–0.013i and 1.49–0.008i respectively at 440 and 675 nm. The volume fraction of BC, BrC, DU, AS and water contents are 1%, 2%, 49%, 15% and 33% respectively. If we only consider dry particle as that is considered in 6S radiative transfer model (Vermeete et al., 1997) and designate BrC and AS

Aerosol physical and chemical properties

Z. Q. Li et al.

Title Page

Abstract

Introduction

Conclusions

References

Tables

Figures

◀

▶

◀

▶

Back

Close

Full Screen / Esc

Printer-friendly Version

Interactive Discussion



as the water-soluble components, the volume fractions of BC, DU, and water-soluble are 1 %, 73 %, and 26 % in the dry particles, respectively over Beijing. In the 6S radiative model, the volume fraction of these three components are 22 %, 70 %, 29 % for urban aerosol type and are 1 %, 70 %, 29 % for continental aerosol type. It can be seen that the aerosol model over Beijing during haze days differs from the standard urban models, but close to the continental model.

4 Discussion

4.1 Comparison with in situ BC measurements

As a preliminary validation, we performed simultaneous aethalometer (Magee Scientific AE51) measurements in February 2012 at our sun-sky radiometer site. The BC mass concentration obtained from AE51 during this period is plotted in Fig. 11, which corresponds to BC content of the surface layer. Another curve represents the column-integrated BC mass concentration retrieved from CE318 under the condition of AOD (440 nm) > 0.4. We employed density of BC (2 g cm^{-3}) as recommend by Bergstrom, 1972) to convert CE318 retrieved volume value to mass concentration. In the comparison, we selected the AE51 measurements within ± 15 min of the CE318 retrievals. From Fig. 11, we can see that the trend of the observed and retrieved BC mass is well correlated, with a correlation coefficient of 0.77. Moreover, the retrieved BC mass can be converted to surface concentration ($\mu\text{g m}^{-3}$) by assuming a uniform BC column height. Conversely, from the good correlation between two curves in Fig. 11, we can estimate that the boundary layer height is about 1 km when comparing surface and column BC concentration. More precisely, the column value from CE318 is slightly lower than the surface value on average, which is consistent with the boundary layer height reported by Zhang et al. (1990), who found the boundary layer height in Beijing is generally less than 1000 m, usually between 500–600 m in winter.

[Title Page](#)[Abstract](#)[Introduction](#)[Conclusions](#)[References](#)[Tables](#)[Figures](#)[◀](#)[▶](#)[◀](#)[▶](#)[Back](#)[Close](#)[Full Screen / Esc](#)[Printer-friendly Version](#)[Interactive Discussion](#)

4.2 Comparison with in situ PM_{2.5} measurements

We compared our observation with in situ hourly PM_{2.5} measurements located in the US Embassy of Beijing (East and south direction from our site, about 10 km) as shown in Fig. 12. From the comparison we found that (1) the heavy haze events have very high PM_{2.5} values from 200 to about 500 mg m⁻³; (2) there are quite good correlation between total column AOD and PM_{2.5}. The correlation coefficient of 0.93 is much higher than that of the averaged conditions when we compare AOD with PM_{2.5} in Beijing. This can be explained by the fact that during heavy haze most of particles are suspended somewhat homogenous in the low level surface and no extra aerosol layers existed; (3) the data yields a linear equation of $PM_{2.5} = 125 \cdot AOD_{500nm} - 79$ which can be used to convert remote sensing observation (e.g. from satellite) to surface PM_{2.5} quantity and could be improved by considering further corrections, like aerosol vertical distribution and ambient humidity.

5 Conclusion

In this paper, we selected two heavy haze events during Beijing winter in 2011 and 2012 to study optical, physical and chemical characterization of haze properties. We summarized a rough selection criteria of AOD (440 nm) > 1.0, $\alpha > 1.0$ and RH < 90 % to select heavy haze condition, based on the ground-based sun-sky radiometer measurements. We used the AERONET aerosol retrieval algorithm to derive single scattering albedo and refractive indices at four wavelengths from 440 to 1020 nm, as well as the particle size distribution of total column aerosols. Then, we employed an improved 5-component (black carbon, brown carbon, mineral dust, ammonium sulfate-like component and aerosol water content) model to retrieve aerosol chemical composition fractions. The model utilized the spectral refractive indices and single scattering albedo, and thus can provide more component information than previous 3 and 4-component models.

Title Page

Abstract

Introduction

Conclusions

References

Tables

Figures

◀

▶

◀

▶

Back

Close

Full Screen / Esc

Printer-friendly Version

Interactive Discussion



Aerosol physical and
chemical properties

Z. Q. Li et al.

Title Page

Abstract

Introduction

Conclusions

References

Tables

Figures

◀

▶

◀

▶

Back

Close

Full Screen / Esc

Printer-friendly Version

Interactive Discussion



Based on the remote sensing observations during haze days in Beijing, a characterization of heavy haze aerosol properties was established, with large AOD of 3.22 at 440 nm and α of about 1.3. The aerosol size distribution was bimodal and the coarse mode occupied a considerable fraction as well. For the refractive indices, the real part exhibited a relatively flat spectral behavior with an average value of about 1.49. The imaginary part showed obviously spectral variation with the value at 440 nm (about 0.013) larger than the other wavelengths (e.g. about 0.008 at 675 nm). The chemical composition retrieval showed that black carbon and brown carbon fractions were not larger than 2 % and 5 % during the haze. Dust and ammonium sulfate-like components were the main contents of the haze aerosols with volume fraction of 49 % and 15 % respectively, while aerosol water content can reach to 33 % in volume. These results can be used in various fields, e.g. improving aerosol remote sensing from satellite, characterization of haze in the environmental and climate models, and correction of aerosol blurring effects for earth observation images from space during the haze condition.

Acknowledgements. This research is supported by National Natural Science Foundation of China (41222007), National Basic Research Program of China (973 Program) under grant 2010CB950800 (2010CB950801), CAS Strategic Priority Research Program (XDA05100200), and European FP-7 Project (ACTRIS). The authors are grateful to aerosol climatology data of Beijing maintained by Hongbin Chen through AERONET, and the US Embassy of Beijing to provide $PM_{2.5}$ observation data.

References

- Arola, A., Schuster, G., Myhre, G., Kazadzis, S., Dey, S., and Tripathi, S. N.: Inferring absorbing organic carbon content from AERONET data, *Atmos. Chem. Phys.*, 11, 215–225, doi:10.5194/acp-11-215-2011, 2011.
- Bäumer, D., Vogel, B., Versick, S., Rinke, R., Mohler, O., and Schnaiter, M.: Relationship of visibility, aerosol optical thickness and aerosol size distribution in an ageing air mass over south-west Germany, *Atmos. Environ.*, 42, 989–998, doi:10.1016/j.atmosenv.2007.10.017, 2008.

Aerosol physical and
chemical properties

Z. Q. Li et al.

Title Page

Abstract

Introduction

Conclusions

References

Tables

Figures

◀

▶

◀

▶

Back

Close

Full Screen / Esc

Printer-friendly Version

Interactive Discussion



Bergstrom, R. W.: Predictions of spectral absorption and extinction coefficients of an urban air-pollution aerosol model, *Atmos. Environ.*, 6, 247–258, doi:10.1016/0004-6981(72)90083-2, 1972.

Bond, T. C. and Bergstrom, R. W.: Light absorption by carbonaceous particles: an investigative review, *Aerosol. Sci. Tech.*, 40, 27–67, 2006.

Dey, S., Tripathi, S. N., Singh, R. P., and Holben, B. N.: Retrieval of black carbon and specific absorption over Kanpur city, northern India during 2001–2003 using AERONET data, *Atmos. Environ.*, 40, 445–456, 2006.

Duan, F. K., Liu, X. D., He, K. B., Li, Y. W., and Dong, S. P.: Characteristics and source identification of particulate matter in wintertime in Beijing, *Water Air Soil Poll.*, 180, 171–183, doi:10.1007/s11270-006-9261-4, 2007.

Dubovik, O., Smirnov, A., Holben, B. N., King, M. D., Kaufman, Y. J., Eck, T. F., and Slutsker, I.: Accuracy assessments of aerosol optical properties retrieved from Aerosol Robotic Network (AERONET) Sun and sky radiance measurements, *J. Geophys. Res-Atmos.*, 105, 9791–9806, doi:10.1029/2000jd900040, 2000.

Dubovik, O., Holben, B., and Thmoas, F. E.: Variability of absorption and optical properties of key aerosol types observed in worldwide locations, *J. Atmos. Sci.*, 59, 590–608, 2002.

Dubovik, O., Sinyuk, A., Lapyonok, T., Holben, B. N., Mishchenko, M., Yang, P., Eck, T. F., Volten, H., Munoz, O., Veihelmann, B., van der Zande, W. J., Leon, J. F., Sorokin, M., and Slutsker, I.: Application of spheroid models to account for aerosol particle non-sphericity in remote sensing of desert dust, *J. Geophys. Res-Atmos.*, 111, D11208, doi:10.1029/2005jd006619, 2006.

He, K. B., Huo, H., and Zhang, Q.: Urban air pollution in China: Current status, characteristics, and progress, *Annu. Rev. Energ. Env.*, 27, 397–431, doi:10.1146/annurev.energy.27.122001.083421, 2002.

Holben, B. N., Eck, T. F., Slutsker, I., Tanre, D., Buis, J. P., Setzer, A., Vermote, E., Reagan, J. A., Kaufman, Y. J., Nakajima, T., Lavenu, F., Jankowiak, I., and Smirnov, A.: AERONET – a federated instrument network and data archive for aerosol characterization, *Remote Sens. Environ.*, 66, 1–16, doi:10.1016/S0034-4257(98)00031-5, 1998.

Lai, L. Y. and Sequeira, R.: Visibility degradation across Hong Kong: its components and their relative contributions, *Atmos. Environ.*, 35, 5861–5872, doi:10.1016/S1352-2310(01)00395-8, 2001.

Aerosol physical and
chemical properties

Z. Q. Li et al.

Title Page

Abstract

Introduction

Conclusions

References

Tables

Figures

◀

▶

◀

▶

Back

Close

Full Screen / Esc

Printer-friendly Version

Interactive Discussion



- Li, Z. Q., Goloub, P., Devaux, C., Gu, X. F., Deuze, J. L., Qiao, Y. L., and Zhao, F. S.: Retrieval of aerosol optical and physical properties from ground-based spectral, multi-angular, and polarized sun-photometer measurements, *Remote Sens. Environ.*, 101, 519–533, doi:10.1016/j.rse.2006.01.012, 2006.
- 5 Li, Z. Q., Blarel, L., Podvin, T., Goloub, P., Buis, J. P., and Morel, J. P.: Transferring the calibration of direct solar irradiance to diffuse-sky radiance measurements for CIMEL Sun-sky radiometers, *Appl. Optics*, 47, 1368–1377, doi:10.1364/Ao.47.001368, 2008.
- Menon, S., Hansen, J., Nazarenko, L., and Luo, Y. F.: Climate effects of black carbon aerosols in China and India, *Science*, 297, 2250–2253, doi:10.1126/science.1075159, 2002.
- 10 Moosmuller, H., Chakrabarty, R. K., and Arnott, W. P.: Aerosol light absorption and its measurement: a review, *J. Quant. Spectrosc. Ra.*, 110, 844–878, doi:10.1016/j.jqsrt.2009.02.035, 2009.
- Nakajima, T. and Tanaka, M.: Algorithms for radiative intensity calculations in moderately thick atmospheres using a truncation approximation., *J. Quant. Spectrosc. Ra.*, 40, 51–69, 1988.
- 15 Nel, A.: Air pollution-related illness: effects of particles, *Science*, 308, 804-806, 2005.
- Okada, K., Ikegami, M., Zaizen, Y., Makino, Y., Jensen, J. B., and Gras, J. L.: The mixture state of individual aerosol particles in the 1997 Indonesian haze episode, *J. Aerosol. Sci.*, 32, 1269–1279, doi:10.1016/S0021-8502(01)00062-3, 2001.
- Russell, P. B., Bergstrom, R. W., Shinozuka, Y., Clarke, A. D., DeCarlo, P. F., Jimenez, J. L., Livingston, J. M., Redemann, J., Dubovik, O., and Strawa, A.: Absorption Angstrom Exponent in AERONET and related data as an indicator of aerosol composition, *Atmos. Chem. Phys.*, 20 10, 1155–1169, doi:10.5194/acp-10-1155-2010, 2010.
- Schuster, G. L., Dubovik, O., Holben, B. N., and Clothiaux, E. E.: Inferring black carbon content and specific absorption from Aerosol Robotic Network (AERONET) aerosol retrievals, *J. Geophys. Res-Atmos.*, 110, D10S17, doi:10.1029/2004jd004548, 2005.
- 25 Schuster, G. L., Dubovik, O., Holben, B. N.: Angstrom Exponent and bimodal aerosol size distributions, *J. Geophys. Res-Atmos.*, 111, D07207, doi:10.1029/2005JD006328, 2006.
- Schuster, G. L., Lin, B., and Dubovik, O.: Remote sensing of aerosol water uptake, *Geophys. Res. Lett.*, 36, L03814, doi:10.1029/2008gl036576, 2009.
- 30 Smirnov, A., Holben, B. N., Eck, T. F., Dubovik, O., and Slutsker, I.: Cloud-screening and quality control algorithms for the AERONET database, *Remote Sens. Environ.*, 73, 337–349, doi:10.1016/S0034-4257(00)00109-7, 2000.

Aerosol physical and
chemical properties

Z. Q. Li et al.

Title Page

Abstract

Introduction

Conclusions

References

Tables

Figures

◀

▶

◀

▶

Back

Close

Full Screen / Esc

Printer-friendly Version

Interactive Discussion



- Stamnes, K., Tsay, S. C., Wiscombe, W., Jayaweera, K.: Numerically stable algorithm for discrete-ordinate-method in multiple-scattering and emitting layered media, *Appl. Optics*, 27, 2502–2509, 1988.
- Sun, Y. L., Zhuang, G. S., Tang, A. H., Wang, Y., and An, Z. S.: Chemical characteristics of PM_{2.5} and PM₁₀ in haze-fog episodes in Beijing, *Environ. Sci. Technol.*, 40, 3148–3155, doi:10.1021/Es051533g, 2006.
- Tan, J. H., Duan, J. C., Chen, D. H., Wang, X. H., Guo, S. J., Bi, X. H., Sheng, G. Y., He, K. B., and Fu, J. M.: Chemical characteristics of haze during summer and winter in Guangzhou, *Atmos. Res.*, 94, 238–245, doi:10.1016/j.atmosres.2009.05.016, 2009.
- Vermote, E., Tanré, D., Deuzé, J. L., Herman, M., and Morcrette, J. J.: Second simulation of the satellite signal in the solar spectrum, 6S: an overview, *IEEE Trans. Geosci. Remote Sens.*, 35, 675–686, 1997.
- Volten, H., Munoz, O., Rol, E., de Haan, J F., Vassen, W., Hovenier, J. W., Muinonen, K., Nouisainen, T.: Scattering matrices of mineral aerosol particles at 441.6 nm and 632.8 nm, *J. Geophys. Res.*, 106, 17375–17401, 2001.
- Wang, L., Li, Z. Q., Li, D. H., Li, K. T., Tian, Q. J., Li, L., Zhang, Y., Lu, Y., and Gu, X. F.: Retrieval of dust fraction of atmospheric aerosols based on spectra characteristics of refractive indices obtained from remote sensing measurements, *Spectrosc. Spect. Anal.*, 32, 1644–1649, doi:10.3964/j.issn.1000-0593(2012)06-1644-06, 2012.
- Wang, L., Li, Z. Q., Tian, Q. J., Ma, Y., Zhang, F. X., Zhang, Y., Li, D. H., Li, K. T., and Li, L.: Retrieval of absorbing black carbon, brown carbon and dust aerosol components from ground-based remote sensing measurements, *J. Geophys. Res.*, submitted, 2013.
- Wu, D., Tie, X. X., Li, C. C., Ying, Z. M., Lau, A. K. H., Huang, J., Deng, X. J., and Bi, X. Y.: An extremely low visibility event over the Guangzhou region: a case study, *Atmos. Environ.*, 39, 6568–6577, doi:10.1016/j.atmosenv.2005.07.061, 2005.
- Yang, M., Howell, S. G., Zhuang, J., and Huebert, B. J.: Attribution of aerosol light absorption to black carbon, brown carbon, and dust in China – interpretations of atmospheric measurements during EAST-AIRE, *Atmos. Chem. Phys.*, 9, 2035–2050, doi:10.5194/acp-9-2035-2009, 2009.
- Yuan, H., Zhuang, G. S., Li, J., Wang, Z. F., and Li, J.: Mixing of mineral with pollution aerosols in dust season in Beijing: revealed by source apportionment study, *Atmos. Environ.*, 42, 2141–2157, doi:10.1016/j.atmosenv.2007.11.048, 2008.

Zhang, A. C., Sun, C. G., and Tian, Y.: Observing results of atmospheric mixed layer in Beijing district and the assessment of theoretical models, *Ac. Meteorol. Sin.*, 48, 345–354, 1990.

ACPD

13, 5091–5122, 2013

Aerosol physical and chemical properties

Z. Q. Li et al.

Title Page

Abstract

Introduction

Conclusions

References

Tables

Figures

⏪

⏩

◀

▶

Back

Close

Full Screen / Esc

Printer-friendly Version

Interactive Discussion



Aerosol physical and chemical properties

Z. Q. Li et al.

Table 1. Typical heavy haze parameter model derived from remote sensing measurements in Beijing winter.

Parameter	Optical properties			Physical properties				Chemical volume fraction				
	AOD (440 nm)	α	SSA (440 nm)	$(r_f (\mu\text{m}), \sigma_f)$ $(r_c (\mu\text{m}), \sigma_c)$	C_f/C_c	(n440, k440)	(n675, k675)	BC %	BrC %	DU %	AS %	AW %
Mean	3.22	1.32	0.91	(0.21, 0.51) (2.90, 0.65)	1.27	(1.48, 0.013)	(1.49, 0.008)	1	2	49	15	33
St.d	0.71	0.13	0.01	(0.030, 0.038) (0.085, 0.007)	0.38	(0.03, 0.002)	(0.03, 0.001)	0	3	11	14	12

(AOD: aerosol optical depth, α : Ångström exponent (440–870 nm), SSA: single scattering albedo, r_f : median radius of fine mode particles, σ_f : standard deviation of fine mode, r_c : median radius of coarse mode particles, σ_c : standard deviation of coarse mode, C_f/C_c : ratio of the fine and coarse particle volume concentration, n : real part of the refractive indices (at 440 and 675 nm, respectively), k : imaginary part of the refractive indices (at 440 and 675 nm, respectively), BC: black carbon, BrC: brown carbon, DU: mineral dust, AS: ammonium sulfate-like, AW: aerosol water).

Title Page

Abstract

Introduction

Conclusions

References

Tables

Figures

◀

▶

◀

▶

Back

Close

Full Screen / Esc

Printer-friendly Version

Interactive Discussion



Aerosol physical and
chemical properties

Z. Q. Li et al.

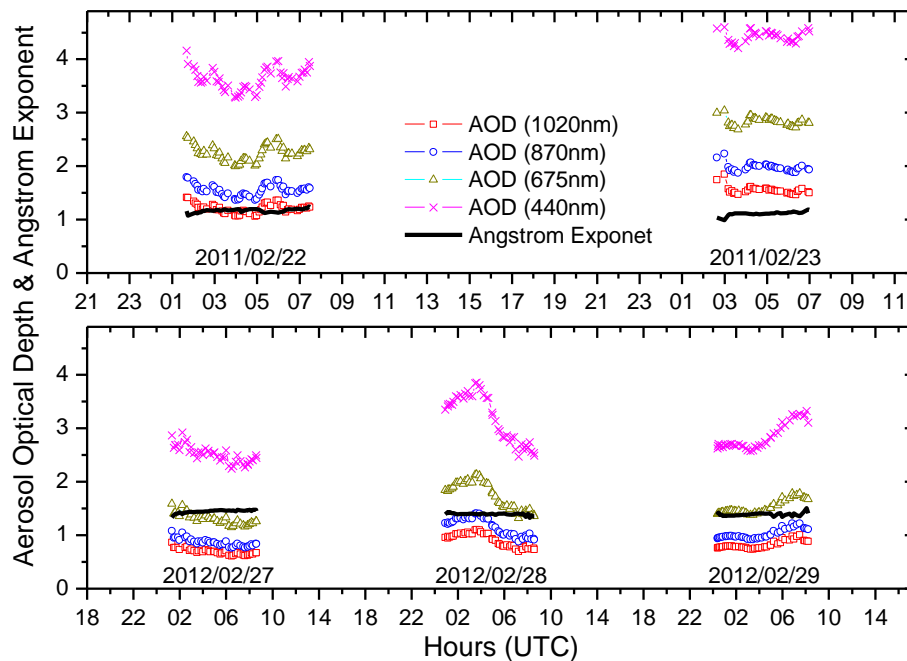


Fig. 1. Time variation of AOD and Ångström exponent (440–870 nm) during two haze events in Beijing.

Title Page

Abstract

Introduction

Conclusions

References

Tables

Figures

◀

▶

◀

▶

Back

Close

Full Screen / Esc

Printer-friendly Version

Interactive Discussion



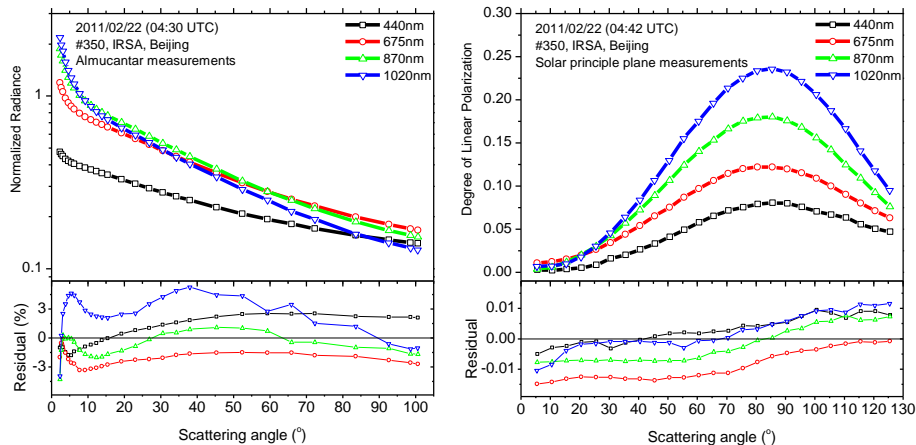


Fig. 2. Fit of the normalized sky radiance and degree of linear polarization by using the retrieved aerosol parameters for haze example on 22 February 2011 in Beijing.

[Title Page](#)[Abstract](#)[Introduction](#)[Conclusions](#)[References](#)[Tables](#)[Figures](#)[◀](#)[▶](#)[◀](#)[▶](#)[Back](#)[Close](#)[Full Screen / Esc](#)[Printer-friendly Version](#)[Interactive Discussion](#)

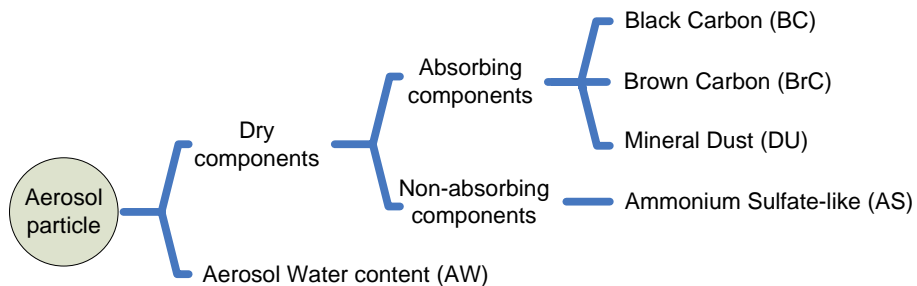


Fig. 3. Aerosol component model used in the chemical composition retrieval.

Aerosol physical and chemical properties

Z. Q. Li et al.

Title Page	
Abstract	Introduction
Conclusions	References
Tables	Figures
◀	▶
◀	▶
Back	Close
Full Screen / Esc	
Printer-friendly Version	
Interactive Discussion	



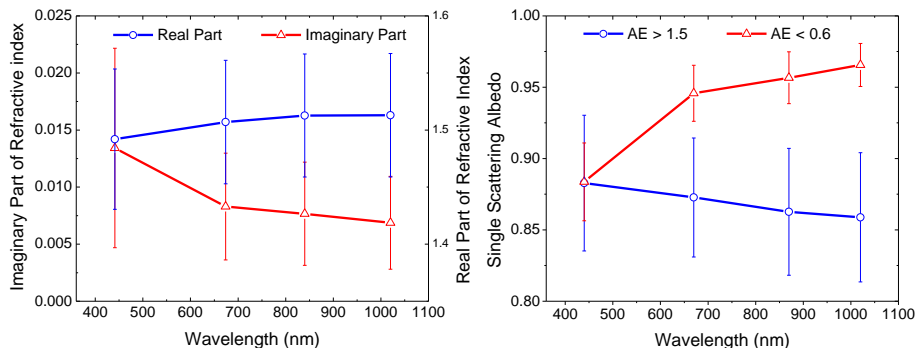


Fig. 4. Averaged aerosol refractive indices (left) and Single Scattering Albedo (right) obtained from sun-sky radiometer measurements from January 2010 to December 2010 in Beijing. The error bar shows the standard deviation and AE on the right panel denotes the Ångström exponent. AE < 0.6 denotes coarse mode dominated cases, while AE > 1.5 denotes fine mode dominated cases.

[Title Page](#)
[Abstract](#)
[Introduction](#)
[Conclusions](#)
[References](#)
[Tables](#)
[Figures](#)
[◀](#)
[▶](#)
[◀](#)
[▶](#)
[Back](#)
[Close](#)
[Full Screen / Esc](#)
[Printer-friendly Version](#)
[Interactive Discussion](#)

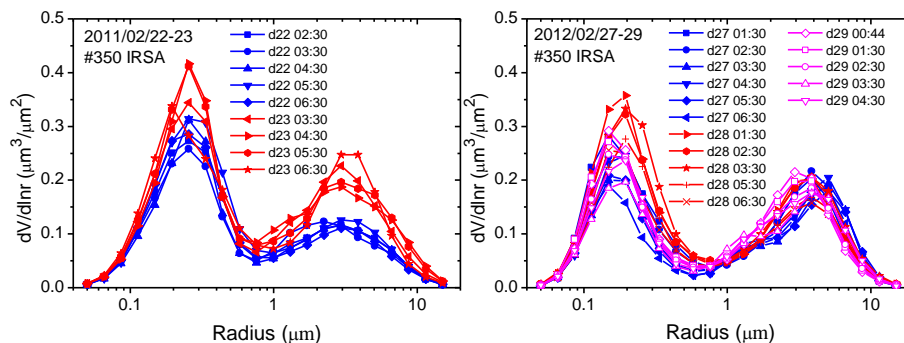



Fig. 5. Aerosol size distribution ($dV/d\ln r$) retrieved in haze day (left: 2011 event, right: 2012 event).

[Title Page](#)
[Abstract](#)
[Introduction](#)
[Conclusions](#)
[References](#)
[Tables](#)
[Figures](#)
[◀](#)
[▶](#)
[◀](#)
[▶](#)
[Back](#)
[Close](#)
[Full Screen / Esc](#)
[Printer-friendly Version](#)
[Interactive Discussion](#)

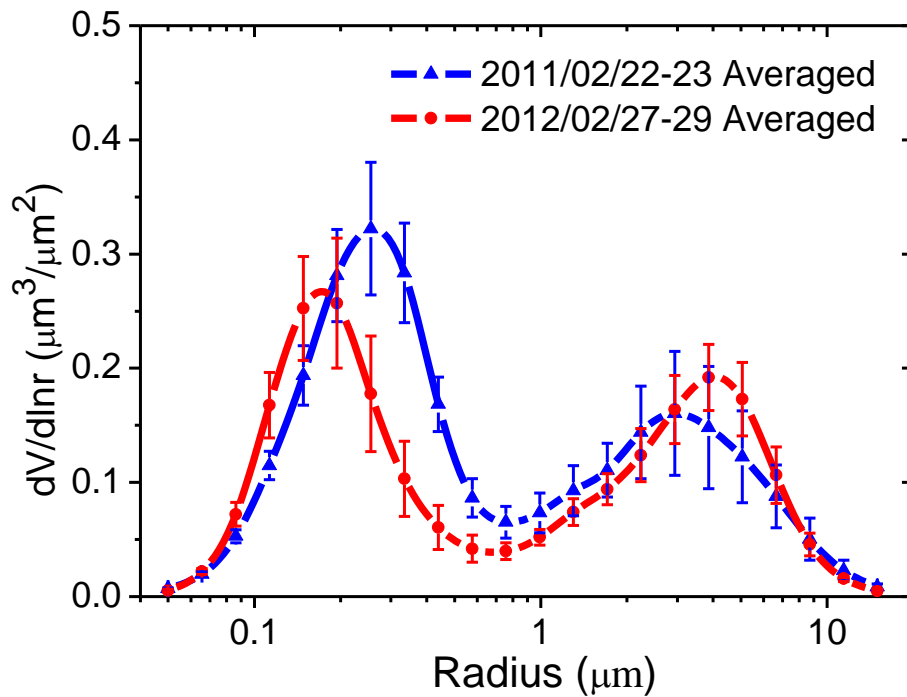



Fig. 6. Comparison of the averaged size distribution of the two haze events in February 2011 and 2012.

[Title Page](#)[Abstract](#)[Introduction](#)[Conclusions](#)[References](#)[Tables](#)[Figures](#)[◀](#)[▶](#)[◀](#)[▶](#)[Back](#)[Close](#)[Full Screen / Esc](#)[Printer-friendly Version](#)[Interactive Discussion](#)

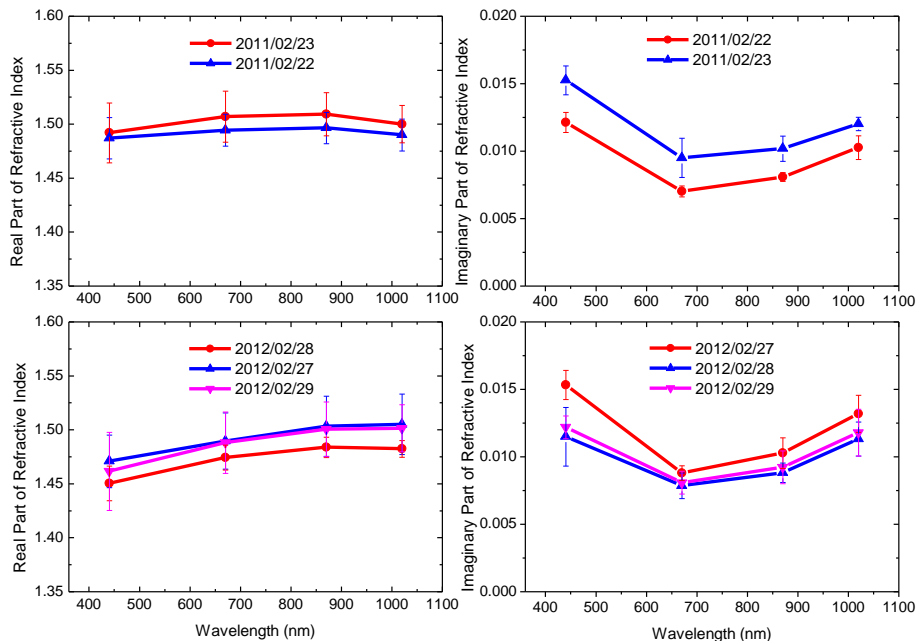


Fig. 7. Daily averaged aerosol refractive index observed in haze days (top: 2011 event, bottom: 2012 event).

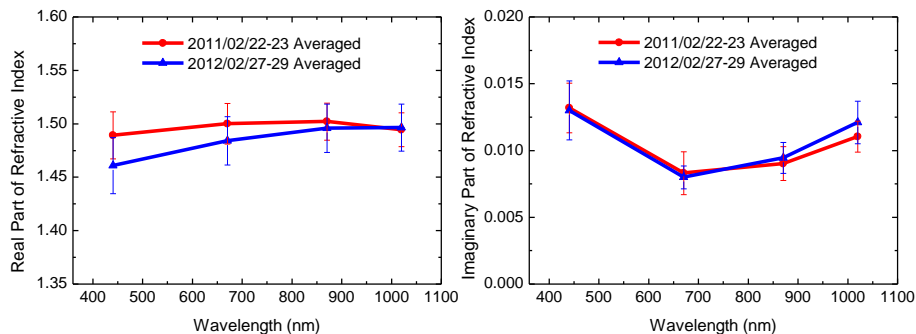


Fig. 8. The averaged refractive index during the haze events in 2011 and 2012 (left: the real parts, right: the imaginary parts).

[Title Page](#)[Abstract](#)[Introduction](#)[Conclusions](#)[References](#)[Tables](#)[Figures](#)[◀](#)[▶](#)[◀](#)[▶](#)[Back](#)[Close](#)[Full Screen / Esc](#)[Printer-friendly Version](#)[Interactive Discussion](#)

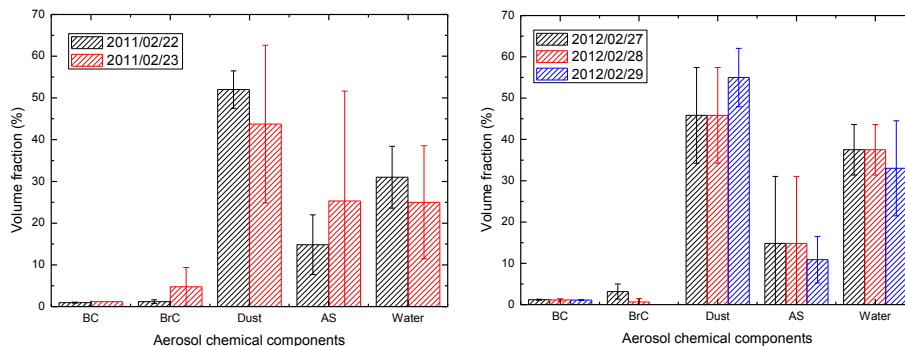


Fig. 9. Daily averaged percentage of aerosol chemical composition (BC: black carbon, BrC: brown carbon, DU: mineral dust, AS: ammonium sulfate-like component, AW: aerosol water content) retrieved during haze days of 2011 (left) and 2012 (right).

[Title Page](#)
[Abstract](#)
[Introduction](#)
[Conclusions](#)
[References](#)
[Tables](#)
[Figures](#)
[◀](#)
[▶](#)
[◀](#)
[▶](#)
[Back](#)
[Close](#)
[Full Screen / Esc](#)
[Printer-friendly Version](#)
[Interactive Discussion](#)

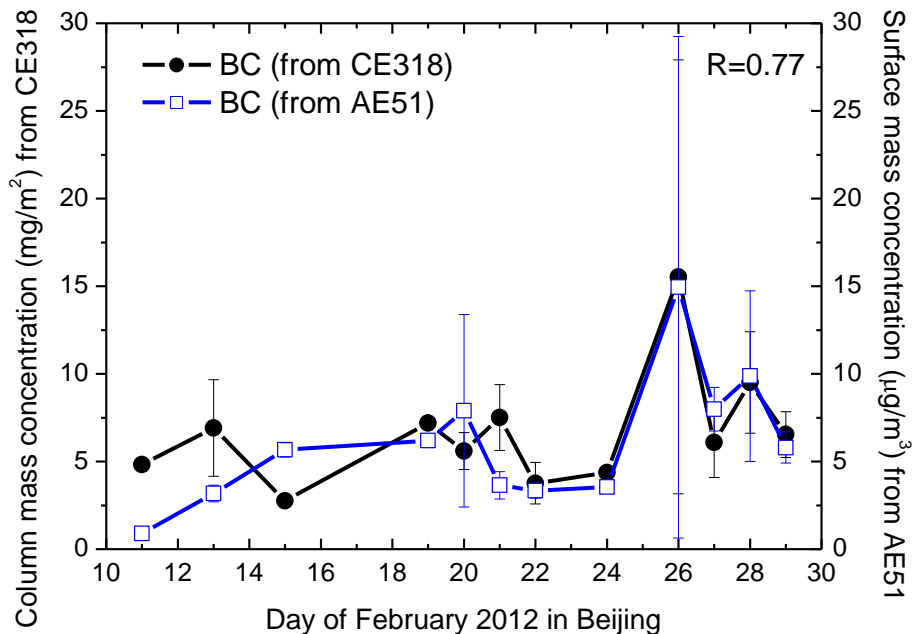



Fig. 11. Daily averaged BC mass concentration obtained from remote sensing retrievals (CE318) and in situ aethalometer measurements (AE51) during February 2012 in Beijing.

[Title Page](#)
[Abstract](#)
[Introduction](#)
[Conclusions](#)
[References](#)
[Tables](#)
[Figures](#)
[◀](#)
[▶](#)
[◀](#)
[▶](#)
[Back](#)
[Close](#)
[Full Screen / Esc](#)
[Printer-friendly Version](#)
[Interactive Discussion](#)

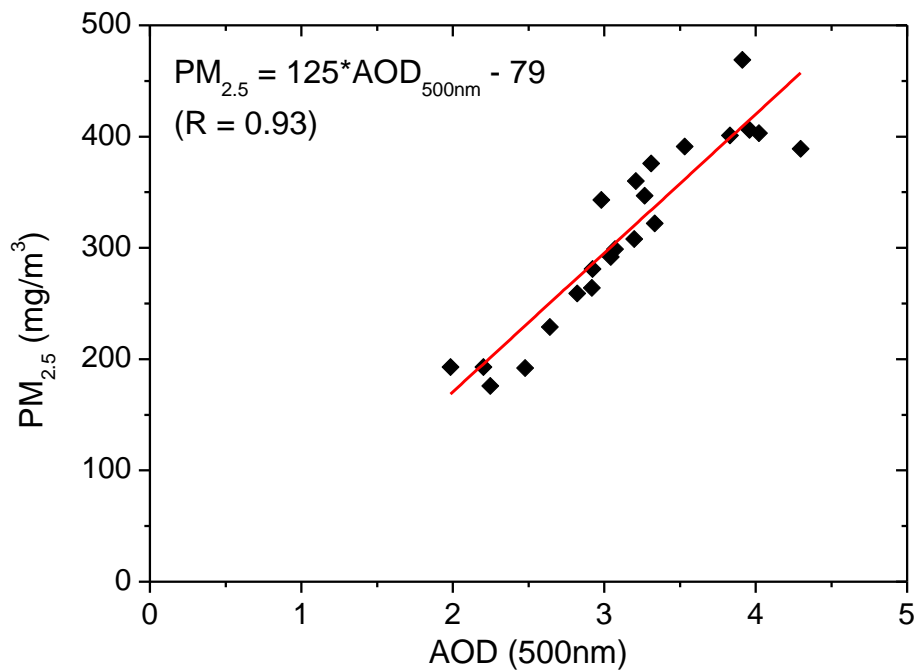



Fig. 12. Comparison of PM_{2.5} with AOD measurements during the two heavy haze events in Beijing winter.

[Title Page](#)[Abstract](#)[Introduction](#)[Conclusions](#)[References](#)[Tables](#)[Figures](#)[◀](#)[▶](#)[◀](#)[▶](#)[Back](#)[Close](#)[Full Screen / Esc](#)[Printer-friendly Version](#)[Interactive Discussion](#)